Biochar

ORIGINAL RESEARCH

Microbial mechanisms of organic matter mineralization induced by straw in biochar-amended paddy soil

Qi Liu[1,2], Cuiyan Wu[3], Liang Wei[1], Shuang Wang[1], Yangwu Deng[4], Wenli Ling[2], Wu Xiang[2], Yakov Kuzyakov[1,5,6,7], Zhenke Zhu[1] and Tida Ge[1*]

Abstract

Combined straw and straw-derived biochar input is commonly applied by farmland management in low-fertility soils. Although straw return increases soil organic matter (SOM) contents, it also primes SOM mineralization. The mechanisms by which active microorganisms mineralize SOM and the underlying factors remain unclear for such soils. To address these issues, paddy soil was amended with ^{13}C-labeled straw, with and without biochar (BC) or fer-rihydrite (Fh), and incubated for 70 days under flooded conditions. Compound-specific ^{13}C analysis of phospholipid fatty acids (^{13}C-PLFAs) allowed us to identify active microbial communities utilizing the ^{13}C-labeled straw and specific groups involved in SOM mineralization. Cumulative SOM mineralization increased by 61% and 27% in soils amended with Straw + BC and Straw + Fh + BC, respectively, compared to that with straw only. The total PLFA content was independent of the straw and biochar input. However, ^{13}C-PLFAs contents increased by 35–82% after biochar addition, reflecting accelerated microbial turnover. Compared to that in soils without biochar addition, those with biochar had an altered microbial community composition-increased amounts of ^{13}C-labeled gram-positive bacteria (^{13}C-Gram +) and fungi, which were the main active microorganisms mineralizing SOM. Microbial reproduction and growth were susceptible to nutrient availability. ^{13}C-Gram + and ^{13}C-fungi increased with Olsen P but decreased with dissolved organic carbon and NO_3^- contents. In conclusion, biochar acts as an electron shuttle, stimulates iron reduction, and releases organic carbon from soil minerals, which in turn increases SOM mineralization. Gram + and fungi were involved in straw decomposition in response to biochar application and responsible for SOM mineralization.

Highlights

- Straw return accelerates microbial mineralization of SOM.
- Combined biochar and straw input raises SOM mineralization by 60%.
- Biochar addition increases ^{13}C incorporation from straw into Gram + bacteria and fungi.
- ^{13}C-Gram + bacteria and ^{13}C-fungi are the dominant active microorganisms that mineralize SOM.

---

*Correspondence:
Tida Ge
getida@nbu.edu.cn
Full list of author information is available at the end of the article

Springer

Graphical Abstract

1 Introduction

With a global cultivation region of nearly 165 million ha, rice paddies have the power to sequester large amounts of soil organic matter (SOM) (Liu et al. 2023; Wei et al. 2022). The increase in SOM storage is essential to maintain soil sustainability and crop yield, provide benefits for agricultural sustainability, and mitigate climate change (Lal 2004; Lehmann and Kleber 2015). Several effective measures were recommended more than 50 years ago to increase carbon (C) stocks in agricultural soils, and these contain organic fertilizer input and straw return. Incorporating organic materials into soils, accelerates SOM mineralization, which may decrease soil C sequestration (Wu et al. 2019; Zhou et al. 2023). Thus, it is key to develop effective measures to raise the share of straw-derived C in the SOM pool and reduce greenhouse emissions.

Biochar application to soils is a promising technology to raise C stocks and decelerate the release of greenhouse gases (Nan et al. 2021). For practical management, straw return combined with biochar application has been extensively utilized considering the balance among plant productivity, soil fertility, and environmental effects (Chen et al. 2022). Despite abundant studies on the role of straw return or biochar incorporation on SOM mineralization in croplands (Jin et al. 2020), details on the effect of biochar on SOM mineralization in paddy soils under anaerobic conditions are lacking. Biochar can function as an electron shuttle owing to the presence of quinone and aromatic structures (Wu et al. 2020). It is also involved in microbially-mediated redox reactions, affecting paddy soil biogeochemical cycling (Liu et al. 2022a). It is imperative to comprehend the microbial mechanisms, by which microbes participate in SOM mineralization induced by straw with biochar-amended paddy soils.

Soil microbes are key drivers of SOM decomposition and nutrient cycling, and distinct microbial species have specific tactics for substrate uptake. For example, gram-negative bacteria (Gram−) preferentially process labile organic matter (OM) sources, but specific gram-positive bacteria (Gram+) and Actinomycetes are important in the decomposition of more complex compounds (Creamer et al. 2015). Fungi are effective in depolymerizing macromolecules (Boer et al. 2005). The transformation of the microbial community structure during rice straw breakdown is influenced by nutrient accessibility and the capacity of microorganism to use soil resources (Zhang et al. 2017). The readily degradable C fraction of substrates might stimulate the growth of Gram−, leading to co-metabolism and a positive priming impact on SOM mineralization (Wang et al. 2015).

Under anaerobic conditions, e.g., in paddy soils, straw addition increased Gram+ lipid fatty acid biomarkers by more than 30%, especially for a15:0 and i15:0, but fungal biomarkers remained stable (Ye et al. 2015). Biochar

input stimulated the development of Actinobacteria (Fu et al. 2022), and the incorporation of fresh biochar increased the content of bacteria (17:1ω8c and i17:0), while aged biochar promoted fungal growth (18:2ω6, 9c) (Liu et al. 2019). Biochar has a very porous structure and can, therefore, provide a shelter for microbial colonization and growth as well as protection from natural enemies (Dai et al. 2021). Manure-derived biochar favored the colonization of Actinomycetes by mycelia and spores (Dai et al. 2017). Further evidence is needed to confirm the roles of bacteria and fungi in SOM decomposition under anaerobic paddy conditions in the presence of straw and straw-derived biochar.

Paddy soils in south China are abundant in iron (hydr) oxides (>17%) (Yu et al. 2016). Unstable iron minerals (especially poorly crystalline Fe oxides) can adsorb and coprecipitate with OM to form extremely chemically strong Fe–OM compounds (Chen et al. 2020). Iron oxides have a greater potential to stabilize SOM in paddy than in dryland ecosystems owing to the frequent redox change that leads to the transformation of iron minerals (Wei et al. 2021), this is particularly true for Fe oxide-enriched rice soils. In addition, changes in the Fe oxide content of paddy soils can affect SOM mineralization. Unstable iron oxides can also alter soil microbial communities through electron exchange processes (Chen et al. 2020). The Fe oxide content in rice soils can both (i) reduce the mineralization of maize-straw-derived C through biotic processes that decrease microbial abundance and activity (such as Actinobacteria and fungi), and (ii) stabilize maize-straw-derived C through abiotic processes that form Fe–OM compounds by co-precipitation (Jeewani et al. 2021). Straw-derived biochar can also serve as an electron shuttle and accelerate iron reduction in paddy soil. This increases the release of mineral bound organic carbon (OC) and the accessibility of OC to microorganisms and their enzymes, which accelerates SOM mineralization (Liu et al. 2022b; Wu et al. 2020). However, it is unclear how changes in Fe oxide contents influence microbial activity and structure in the presence or absence of biochar.

We aimed to investigate the microbial mechanisms underlying straw-induced SOM mineralization after biochar application in anaerobic paddy soils. We hypothesized that (a) biochar application increases Fe reduction rates and C availability, which further increases microbial activity and SOM mineralization, and (b) the abundance and structure of the microbial community changes with straw decomposition, which affects SOM mineralization. To examine these hypotheses, we first used ^{13}C-labeled straw to trace C sources in mineralized CO_2 and phospholipid fatty acids (PLFAs) of soil microbes. We subsequently investigated the active microbial communities

participating in SOM mineralization as well as the main influencing factors. Ferrihydrite was applied to imitate weakly crystalline iron oxides, whereas straw-derived biochar was applied to mimic biochar derived from straw burning in paddy soil.

2 Materials and methods

2.1 Research sites and soil sampling

Soils were taken from the surface layer (0–20 cm) of rice fields in Jinjing Township, Changsha City, Hunan Province (113°19′ 52″ E, 28°33′ 04″ N), which were classified as Stagnic Anthrosols that originated from quaternary red clay. This study area has a humid subtropical climate with a mean annual temperature of 17 °C and yearly rainfall of 1300 mm. The sampled soil was moved to the laboratory, and visible crop debris and rocks were manually discarded. A portion of the soil samples was air-dried and sieved (2 mm mesh sieve) for physicochemical analysis. Other portions were submerged and precultivated for 14 days in a greenhouse. The fundamental physicochemical characteristics of the soil collected for the study can be found in Liu et al. (2022a).

2.2 Preparation of ^{13}C-labeled rice straw, biochar, and ferrihydrite

The ^{13}C-labeled straw was obtained with reference to the approach elaborated by Zhu et al. (2017). The detailed preparation process of straw and the measuring apparatus are given in Additional file 1: Method S1. Ultimately, the isotope abundance of ^{13}C in straw was on average 2.54 atom%.

Biochar was generated by a company in Shanxi, China, whose technology focuses on producing bioenergy. It was formed by pyrolysis of rice straw at 550 °C for 7 h under anaerobic conditions in a muffler furnace. After 7 h of heating, the biochar samples were cooled to 18–25 °C. The biochar had a pH of 9.3 (1:10 w/v), and total C, total N, and total ash levels of 42, 0.6, 37%, respectively.

Ferrihydrite (Fh) was prepared in accordance with the procedures described in Das et al. (2011). In summary, $FeCl_3 \cdot 6H_2O$ was dissolved in double-distilled deionized (DDI) water to achieve a concentration of 0.4 M and then titrated with 1 M NaOH to achieve a pH of 7–8. The supernatant obtained was centrifuged and then cleaned using deionized water. The stock suspension of ferrihydrite was stored in a fridge and applied within 3 days.

2.3 Soil incubation

Each of the four treatments with the addition of labeled straw was accompanied by a control treatment without straw, thus this trial totally involved eight amendments with three replications each. Details of the experimental design, including information on the used materials and

isotope abundance of ^{13}C in straw, are shown in Table 1. Additionally, we set up treatments with unlabeled straw addition to test the natural abundance of ^{13}C. We separately poured 150 g of pre-cultured soil (equal to 100 g of dry soil) into 500 mL serum and plastic bottles for subsequent independent testing of gas and soil samples. The straw amendment bottles were uniformly treated with 1.5 g C kg^{-1} dry soil of ^{13}C-labeled straw (2.54 atom% ^{13}C). Furthermore, BC and Fh amendments were applied to bottles at rates of 10 g biochar kg^{-1} dry soil and 1.76 g Fe kg^{-1} dry soil, respectively. To simulate flooding conditions in a paddy field, deionized water (100 mL) was poured into the bottles to attain a water level of 2–3 cm. These glass bottles were sealed with a butyl rubber stopper and purged with pure N_2 gas for 20 min, and then incubated for 70 days in a greenhouse.

2.4 CO$_2$ and CH$_4$ collection and analysis

Gas production was usually more rapid in the initial 28 days and subsequently decelerated gradually to the pre-experiment levels. Gas collection was performed at specific intervals of 1, 3, 5, 7, 10, 14, 21, 28, 35, 42, 49, 56, 63, and 70 days of incubation. During each sampling session, air was picked up using a 30 mL gas-tight syringe and saved in a serum bottle that had been evacuated and capped with butyl rubber stoppers. Gas samples were determined using an Agilent 7890A gas chromatograph (Agilent Technologies, Palo Alto, CA, USA). We used an isotope ratio mass spectrometer combined with a Gasbench instrument (Thermo Fisher Scientific, Waltham, MA, USA) to determine the steady C isotope components of CO_2 and CH_4.

$$^{13}C\text{-MBC} = [\left(\text{atom\% } ^{13}C_{fu, la} - \text{atom\% } ^{13}C_{fu, ula}\right) \times C_{fu} - \left(\text{atom\% } ^{13}C_{nfu, la} - \text{atom\% } ^{13}C_{nfu, ula}\right) \times C_{nfu}] \Big/ (100 \times 0.45), \tag{2}$$

According to the approach introduced by Phillips et al. (2005), we used an end-member mixing model to compute the fraction of SOM-derived C from CO_2/CH_4 (C_{SOM}) as follows:

$$C_{SOM} = C_{overall} \times \left(\text{atom\% } ^{13}C_{overall} - \text{atom\% } ^{13}C_{straw}\right) \Big/ \left(\text{atom\% } ^{13}C_{SOM} - \text{atom\% } ^{13}C_{straw}\right), \tag{1}$$

where atom% $^{13}C_{overall}$, atom% C_{straw}, and atom% C_{SOM} are the atomic percentages of ^{13}C values in overall CO_2/CH_4 emitted from the straw-amended groups, overall CO_2/CH_4 originating from the added straw, and overall CO_2/CH_4 emitted from the bulk soil, respectively (Phillips et al. 2005). The following calculation was then used: mineralization rate of the straw (%) = amount of

Table 1 Basic information for each experimental treatment

Treatments	Straw (g kg^{-1})	^{13}C atom % of straw	Ferrihydrite (g kg^{-1})	Biochar (g kg^{-1})
(1) Soil (control)	–	–	–	–
(2) Straw	1.5	2.54	–	–
(3) Soil + BC	–	–	–	10
(4) Straw + BC	1.5	2.54	–	10
(5) Soil + Fh	–	–	3.4	–
(6) Straw + Fh	1.5	2.54	3.4	–
(7) Soil + BC + Fh	–	–	3.4	10
(8) Straw + BC + Fh	1.5	2.54	3.4	10

CO_2 and CH_4 emitted by the straw/initial ^{13}C amount of straw × 100%, and mineralization rate of SOM (%) = C_{SOM}/SOC × 100%.

2.5 Soil chemical and microbial properties analyses

Soil was destructively sampled from individual bottles at 3, 28, and 70 days to analyze soil microbial properties. Soil microbial biomass C (MBC) and dissolved organic carbon (DOC) extracted with 0.5 M K_2SO_4 were quantified using the chloroform fumigation extraction approach (Wu et al. 1990). The $^{13}C/^{12}C$ values were then determined employing an isotope ratio mass spectrometer (MAT253), equipped with an elemental analyzer (FLASH 2000; Thermo Fisher Scientific). Then, we calculated the $\delta^{13}C$ value of MBC as follows (Ge et al. 2012):

where fu, nfu, la, and ula represent fumigated, non-fumigated, labeled, and unlabeled soil extracts, respectively. C_{fu} and C_{nfu} separately denote the total OC levels of the fumigated and non-fumigated soil extracts.

The determination methods of soil nitrate nitrogen (NH_4^+), ammonium nitrogen (NO_3^-), available phosphorus (Olsen P) and Fe^{2+} concentration are provided in Liu et al. (2022a). Extracellular hydrolytic enzyme activities were examined using fluorogenic methylumbelliferone-based artificial substrates as described in Additional file 1: Method S2.

2.6 Soil microbial PLFA analysis

Extraction, fractionation and purification of soil microbial PLFAs were performed according to the protocol proposed by Yuan et al. (2016). More details are given in Additional file 1: Method S3.

The following PLFAs biomarkers were used to identify specific microbial clusters: i14:0, i15:0, a15:0, i16:0, i17:0, and a17:0 for Gram +, and 16:1 ω7c, 17:1 ω8c, 18:1 ω7c, cy17:0, and cy19:0 for Gram − (Zelles 1999). Biomarkers for fungi were 18:1 ω9c, 18:2 ω6c, and 16:1 ω5c (Bååth and Anderson 2003), whereas 10Me16:0, 10Me17:0, 10Me17:1 ω7c, 10Me18:1 ω7c, and 10Me18:0 PLFAs biomarkers were used as a biomarker for Actinomycetes (Act). Non-specific (universal) PLFAs included 14:0, 15:0, 16:0, 17:0, 18:0, and 20:0, which also contribute to the total PLFA content (Zhu et al. 2022). Despite accounting for only a little fraction of the whole biomass, PLFAs can be applied as an indicator of the active microbial biomass (Zhang et al. 2019). In this work, we applied PLFA analysis to measure shifts in microbial biomass and compare the ingestion of labeled substrates among the various microbial taxa.

The quantity of ^{13}C integration in various PLFAs (mg kg^{-1}) was calculated utilizing a mass balance method as follows:

PLFAs in each particular microbial taxon was calculated using the following equation (Tian et al. 2013):

$$^{13}C\% = {}^{13}C_{PLFA\text{-}taxon} \Big/ \Sigma {}^{13}C_{PLFA} \times 100, \quad (4)$$

where $^{13}C_{PLFA\text{-}taxon}$ is the value of ^{13}C-PLFAs integrated into each particular microbial taxon and $\sum{}^{13}C_{PLFAs}$ is the overall value of ^{13}C-PLFAs integrated into soil microbes.

2.7 Statistical analyses

All statistical analyses were performed and all figures generated utilizing the R software (version 4.2.1; http://www.r-project.org/). One-way analysis of variance was applied to determine differences between samples at the same sampling point, followed by the Duncan's multiple range test to identify significant differences between individual treatments. The absolute content of ^{13}C in PLFAs was computed and subsequently normalized to a variance of 1 to create a correction matrix for principal component analysis (PCA). Spearman correlation and regression analyses were conducted to evaluate the relationship among soil geochemical attributes, extracellular enzyme activity, and ^{13}C-PLFAs of soil microbial groups using the "rcorr" package and "lm" function, respectively. A random forest (RF) model was then performed to estimate the contribution of soil
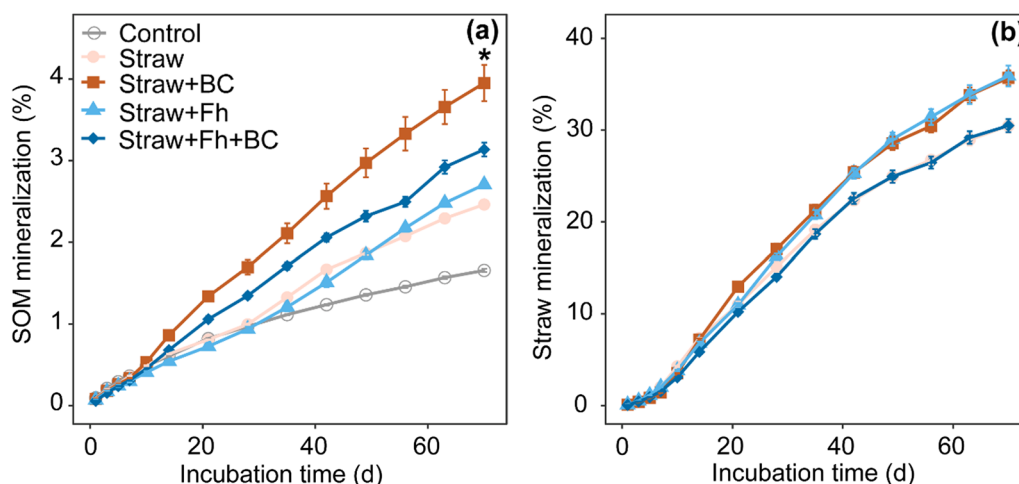
$$^{13}C_{PLFA} = \left(atom\% \, {}^{13}C_{PLFA,\,La} - atom\% \, {}^{13}C_{PLFA,\,ULa} \right) \Big/ 100 \times C_{PLFA}, \quad (3)$$

where atom%$^{13}C_{PLFA,\,La}$ and atom%$^{13}C_{PLFA,\,ULa}$ represent the PLFA extracts from the labeled and unlabeled groups, respectively. The proportion of ^{13}C relative to the total

properties and extracellular enzyme activity in explaining the ^{13}C enrichment in PLFAs. The relation of each predictor with respect to the dependent variables was

Fig. 1 Cumulative mineralization of soil organic matter (SOM) (**a**) and straw (**b**) in response to biochar (BC) and ferrihydrite (Fh) application during 70 days of incubation. Error bars indicate the standard deviation (n = 3). Asterisk indicate significant differences between amendments at the end of incubation (*$p < 0.05$)

evaluated using the "rfPermute" package. We also performed regression analysis to assess the effects of ^{13}C-PLFAs of soil microbial groups and abiotic indicators on SOM mineralization. The contributions of biotic and abiotic indicators and the absolute content of individual ^{13}C-PLFAs to SOM mineralization were predicted using RF analysis.

3 Results

3.1 SOM and straw mineralization

Straw addition accelerated SOM mineralization compared to the amendment without straw ($p < 0.05$, Fig. 1a). The application of straw combined with biochar led to faster SOM mineralization compared to that with only straw addition ($p < 0.05$). The cumulative SOM mineralization was 2.5% with only straw, whereas adding biochar or biochar and ferrihydrite increased

SOM mineralization by 61 and 27%, respectively. Straw mineralization was impacted by the incorporation of biochar or ferrihydrite, and the cumulative straw mineralization was increased by 18% in the soil with Straw + BC and Straw + Fh compared to that with the straw-only amendment (Fig. 1b).

3.2 Dynamics of straw-derived C incorporated into MBC and PLFAs

The ^{13}C-DOC dynamics were similar for all treatments during the 70-day incubation, but the incorporation of straw into DOC sharply decreased from 35 to 3.5 μg C kg^{-1} (Fig. 2a). The maximum amount of ^{13}C-MBC was obtained in the Straw + Fh + BC group (Fig. 2b). The microbial turnover rate (based on ^{13}C in MBC) decreased sharply during the incubation period for all four amendments. Straw + Fh + BC resulted in the fastest microbial
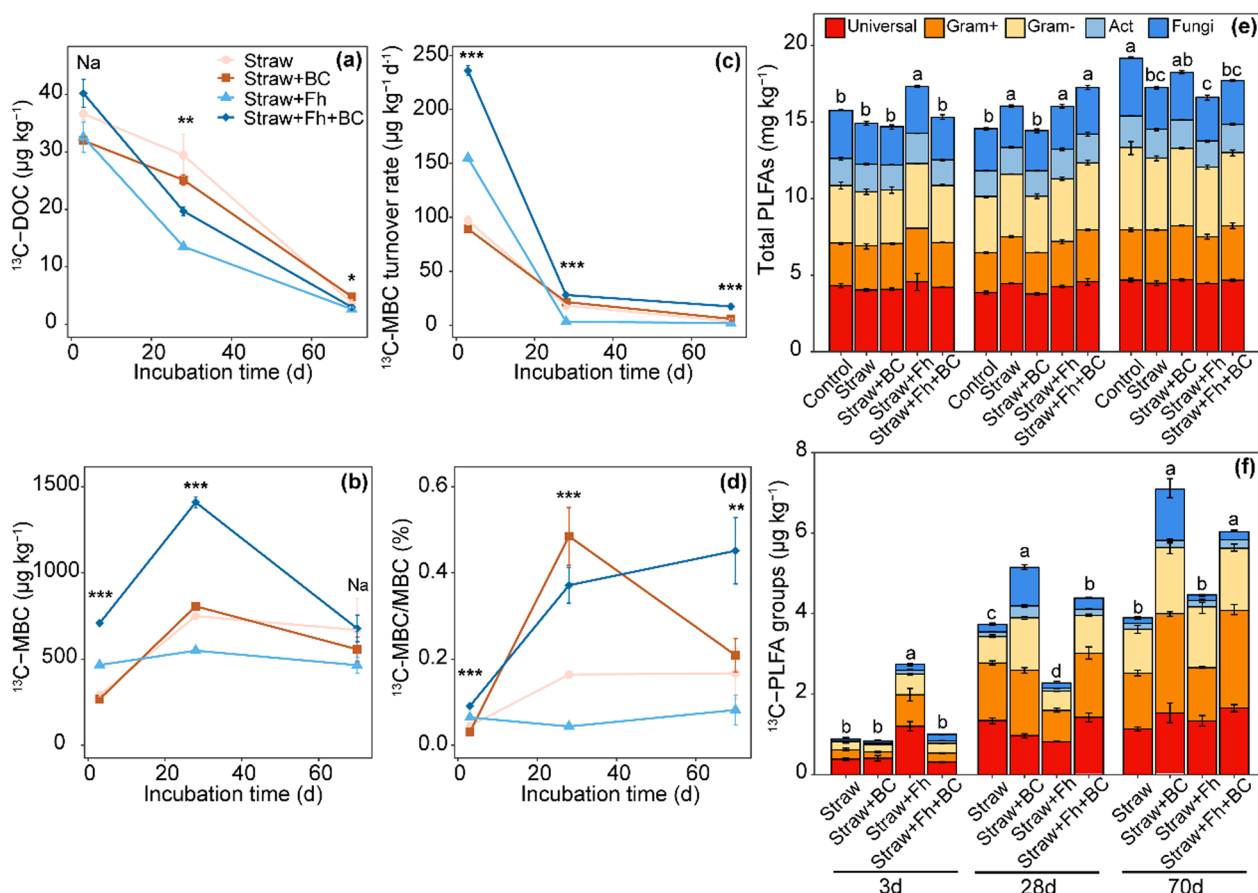

Fig. 2 Dynamics of ^{13}C-labeled dissolved organic carbon (^{13}C-DOC) (**a**), the content and turnover rate of ^{13}C-labeled microbial biomass carbon (^{13}C-MBC) (**b**, **c**), the proportion of ^{13}C-MBC in total microbial biomass (**d**), phospholipid fatty acid (PLFA) contents of each microbial group in soil during incubation (**e**), and ^{13}C-labeled phospholipid fatty acid (^{13}C-PLFA) content of each microbial group for 70 days of incubation (**f**). PLFAs were defined as non-specific (universal), gram-positive bacteria (Gram +), gram-negative bacteria (Gram −), Actinomycetes (Act), and fungi. Values suggest the mean ± standard error (n = 3), Asterisk indicate significant differences between amendments at the same point in time (*$p < 0.05$, **$p < 0.01$, ***$p < 0.001$); Na indicate no significant difference between treatments at each sampling period. Lowercase letters illustrate significant differences at $p < 0.05$ among amendments at each sampling period

turnover rate after 3 days of incubation, followed by Straw + BC (Fig. 2c). Biochar increased the proportion of ^{13}C-MBC in total microbial biomass (Fig. 2d).

The total PLFA level ranged from 14 to 19 mg C kg^{-1} throughout the incubation, which was increased by an average of 6.1% in biochar-treated soils (17–18 mg C kg^{-1}) compared to that in soils without biochar (16–17 mg C kg^{-1}) by day 70 (Fig. 2e, p > 0.05). The total ^{13}C-PLFA content in the soil with straw and ferrihydrite (Straw + Fh) remained stable, but the ^{13}C in total PLFAs increased during the incubation ($p < 0.01$). The total ^{13}C-PLFA content in the Straw + BC and Straw + Fh + BC groups increased by 82 and 35%, respectively, compared to that in the Straw and Straw + Fh groups after the 70-day incubation (Fig. 2f). Straw-derived C was unevenly distributed among microbial groups, indicating their different capacities for straw utilization. Biochar addition increased the ^{13}C incorporation into PLFAs in comparison to no biochar addition. Specifically, the absolute levels of ^{13}C-Gram +, ^{13}C-Act, and ^{13}C-fungi in the soils treated with biochar increased by 77–84%, 27–34%, and 42–790%, respectively, when compared to the soils without biochar application. Biochar addition affected the capacity of microorganisms to assimilate nutrients and regulated microbial activities in soil. The ^{13}C-PLFA content decreased with DOC, ^{13}C-DOC, and NO$_3^-$, but increased with Olsen P (Fig. 3a–d). Additionally, the

contents of ^{13}C-fungi, ^{13}C-Gram +, and ^{13}C-Act also decreased with DOC, ^{13}C-DOC, and NO$_3^-$, but increased with Olsen P (Additional file 1: Fig. S1). Random forest models further showed that the levels of DOC, NO$_3^-$, and Olsen P were the most important predictors of ^{13}C-PLFAs (Fig. 3e, p < 0.001).

3.3 Linking labeled microbial groups, soil geochemical attributes, and enzyme activities to SOM mineralization

The ^{13}C-PLFAs of microbial groups and abiotic soil properties affected SOM mineralization. The SOM mineralization increased with the relative content of ^{13}C-PLFAs, ^{13}C-Gram +, and ^{13}C-fungi (Fig. 4a–f, p < 0.05). Random forest analysis further demonstrated that the contributions of ^{13}C-fungi and ^{13}C-Gram + to SOM mineralization were higher than those of ^{13}C-Gram −, and the levels of ^{13}C-DOC, NO$_3^-$, DOC, and Olsen P were the main variables that predicted SOM mineralization (Fig. 4g, p < 0.001).

A PCA plot was created to examine the impact of the treatments on the microbial community composition (Fig. 5a). The first and second principal components separately contributed 51 and 27% to the entire variance in the microbial population. The biochar-amended soils (Straw + BC and Straw + Fh + BC) were unequivocally distinguished from the soil without biochar (Straw
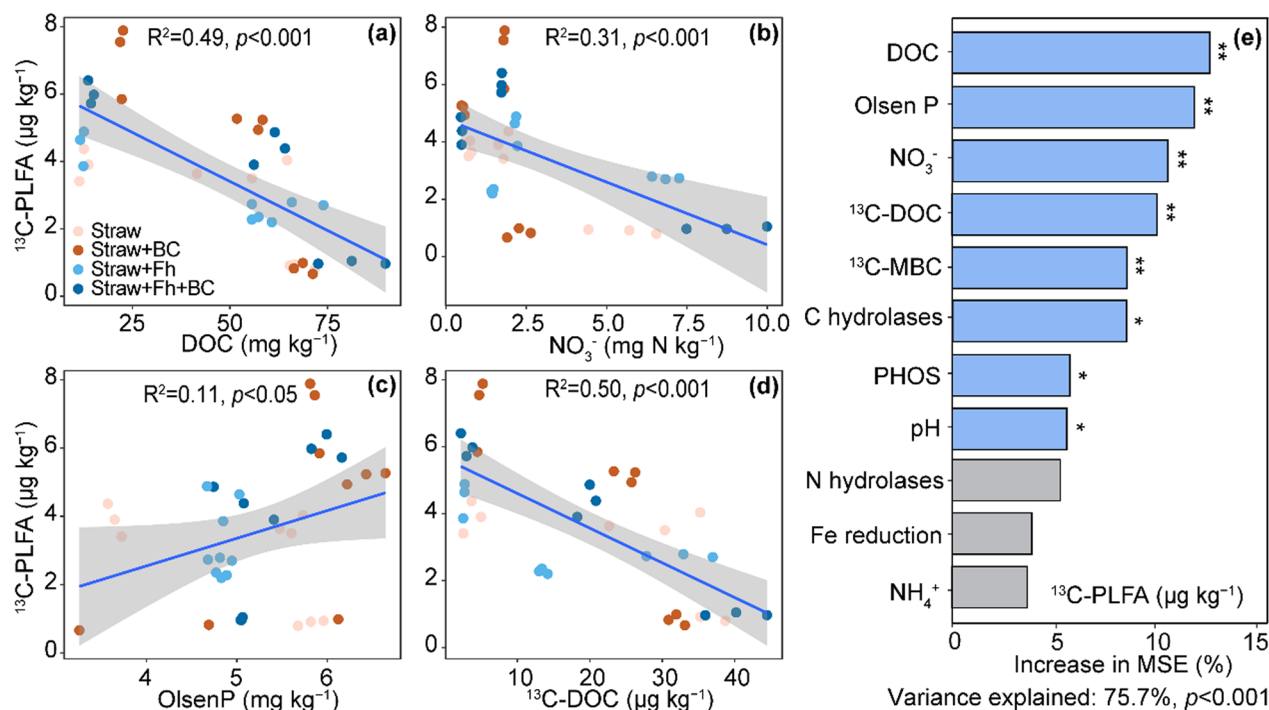

Fig. 3 Regressions between available soil resources and ^{13}C-labeled phospholipid fatty acids (^{13}C-PLFA) (**a–d**). Mean predictor of important factors related to ^{13}C-PLFA based on random forest analysis (**e**). The blue bars demonstrate significance (*p < 0.05, **p < 0.01). *MSE* mean square error
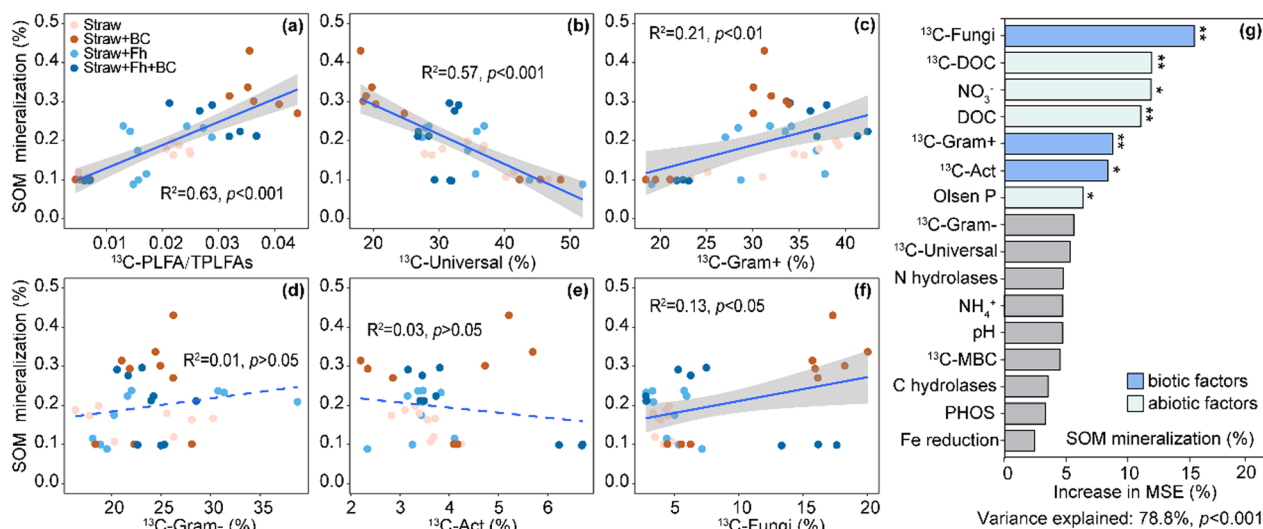
Fig. 4 Regressions between biomarkers of microbial groups and SOM mineralization (**a–f**). The contribution of biomarkers of microbial groups and soil properties to SOM mineralization was investigated using a random forest model (**g**). The colored bars separately indicate biotic and abiotic factors (*$p < 0.05$, **$p < 0.01$). *MSE* mean square error
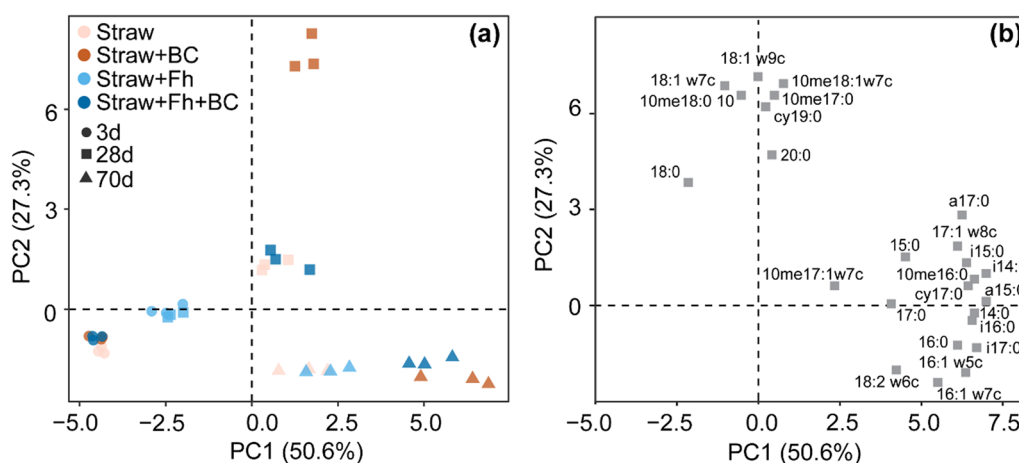

Fig. 5 Principal component analysis according to the absolute contents of individual ^{13}C-labeled phospholipid fatty acids (^{13}C-PLFAs) derived from straw in the soil (**a**) and (**b**) loading plot. The proportion of variance explained is shown on each axis. Colors indicate the amendments, symbols indicate time

and Straw + Fh) after the 70-day incubation period. The Straw + BC and Straw + Fh + BC groups received higher scores along PC1 than those with the corresponding amendments without biochar after 3 days of incubation (Fig. 5a). The factor scores of single PLFAs on PC1 revealed that the ^{13}C-PLFAs i17:0, i16:0, 16:1 w5c, and 18:2 ω6c gathered in the biochar-amended soil after 70 days (Fig. 5b).

Seventeen PLFA biomarkers were identified from the labeled straw-derived C. The absolute contents of individual straw-derived ^{13}C-PLFAs in the Straw + Fh soil remained stable, except for the increase in the individual

^{13}C-PLFAs with other amendments over time (Fig. 6a–c). Labeled straw-derived C was mainly assimilated into 16:1 w7c, followed by 16:0, a15:0, and i15:0, after 70 days of incubation. The absolute contents of the ^{13}C-PLFAs a15:0, i15:0, i16:0, a17:0, and i17:0 (Gram +), and 16:1 w5c and 18:2 ω6c (fungi) were greater in the groups amended with biochar than in those without biochar (Fig. 6c). The RF models further suggested that the contribution of the individual ^{13}C-PLFAs i17:0, i16:0, 16:1w5c, 18:1 w9c, 16:1 w7c, and cy17:0 to SOM mineralization was high (Fig. 6d, p < 0.001).
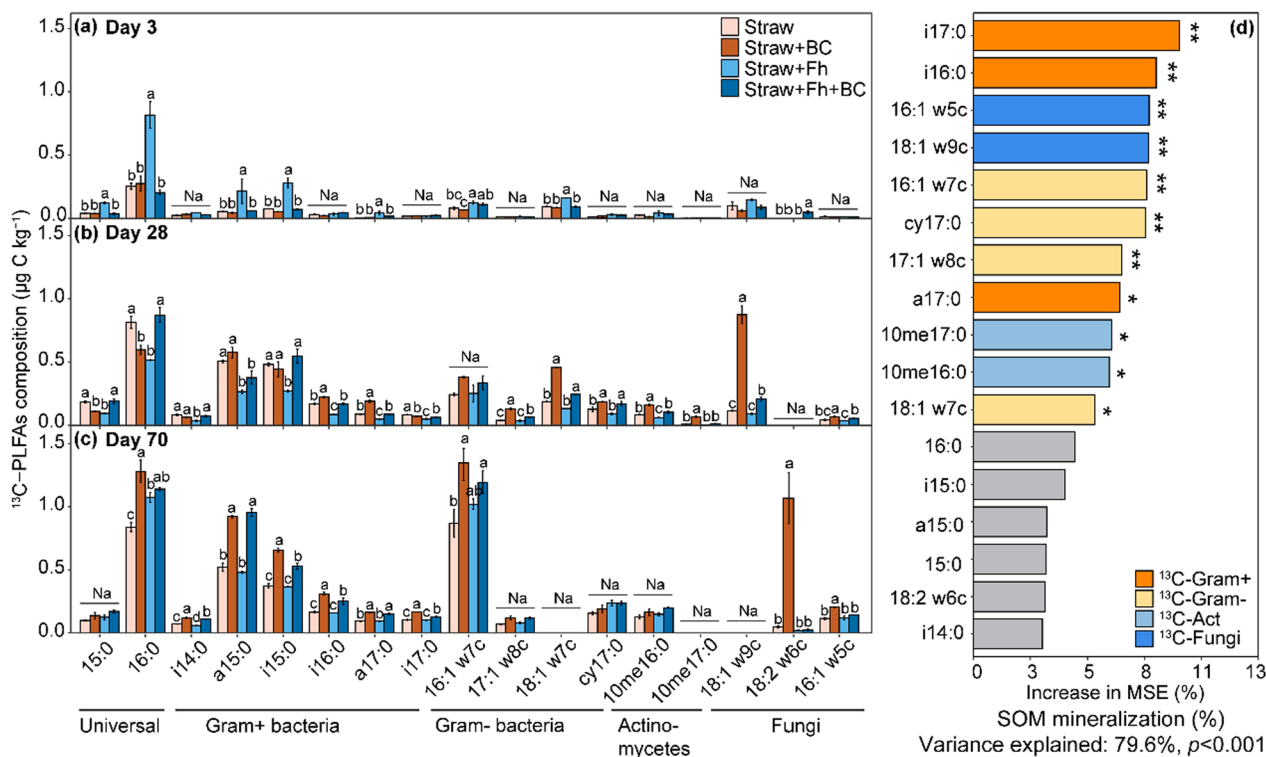
Fig. 6 Absolute contents of individual ^{13}C-labeled phospholipid fatty acids (^{13}C-PLFAs) derived from straw (**a**–**c**). The contribution of the absolute contents of individual ^{13}C-PLFAs to soil organic matter (SOM) mineralization was studied using a random forest model (**d**). Vertical bars denote the standard errors of the means. Lowercase letters illustrate significant differences at $p < 0.05$ among amendments at each sampling period. Na indicates no significant differences between treatments at each sampling period. The colored bars indicate various microbial groups (*$p < 0.05$, **$p < 0.01$)

4 Discussion

4.1 Effects of ferrihydrite and biochar on SOM mineralization

SOM mineralization was originally reduced by straw incorporation during the early phase of incubation (20 days) but then gradually increased as the labile C depleted (Fig. 1a). The early phase of fast CO_2 release was induced by the decomposition of labile organic substances from straw. SOM mineralization increased by 61% with biochar addition (Straw + BC) compared to that with the addition of straw alone (Fig. 1a). The nutrients (N and P) contained in biochar could increase microbial growth and activity (Mukherjee et al. 2020), thereby accelerating SOM mineralization (Sheng and Zhu 2018). Olsen P and NH_4^+ levels were greater in the soil treated biochar than in soils without biochar input (Additional file 1: Fig. S2).

The RF analysis also indicated that the levels of DOC, Olsen P, and NO_3^- were the most important predictors of SOM mineralization (Fig. 4g), suggesting that available nutrients are key determinants of microbial colonization and growth (Marschner et al. 2011). Consequently, the increase in available nutrient contents due to biochar

inputs raised microbial biomass, which facilitated SOM utilization. In contrast, the lowest SOM mineralization in the Fe-rich soils (Straw + Fh) during the first 28 days of incubation was attributed to ferrihydrite characteristics, including its large surface area and sorption capacity (Chen et al. 2014). Consequently, ferrihydrite adsorbed labile C, causing a decline in the available C pool, which ultimately reduced the microbial utilization of SOM (Cooper et al. 2017; Jilling et al. 2021). Biochar addition, however, increased SOM mineralization by 16% compared to that with Straw + Fh group. This is because biochar acts as an electron shuttle under anaerobic conditions (Chen et al. 2016; Yu and Kuzyakov 2021), which increases the reductive dissolution of ferrihydrite and diminishes the protective effects of Fe oxides on SOM (Keiluweit et al. 2015), thus increasing microbial accessibility of SOM (Pan et al. 2016). This phenomenon upholds our hypothesis that biochar application increases iron reduction and OC availability, in turn facilitating microbial activity and SOM mineralization. This was confirmed by the fact that Fe reduction was more prevalent in the Straw + Fh + BC group than in the group without biochar (Straw + Fh) (Additional file 1: Fig. S2e).

Consequently, SOM mineralization was more intensive with biochar than with ferrihydrite.

4.2 Microbial mechanisms of SOM mineralization induced by straw in response to biochar application

Straw return is a large source of C and energy to stimulate microbial maintenance and growth, thus facilitating microbial diversity and the community modification (Su et al. 2020). The united incorporation of straw and biochar further increased microbial richness and altered the constitution of the microbial community (Li et al. 2018; Palansooriya et al. 2019). The overall PLFA level in the soil with biochar was only 6.1% larger than that without biochar (Fig. 2e, p > 0.05), indicating that biochar was not a C source for microbial growth and did not have a direct effect on microbial abundance. Although microorganisms cannot utilize biochar due to its recalcitrance, biochar with a high surface area can adsorb nutrients and soluble OC, thereby accelerating microbial colonization (Singh et al. 2022). The adaptive evolution and colonization of the microbial population in response to the incorporated biochar, in turn, may have further contributed to the microbial C utilization efficiency of straw. Therefore, biochar incorporation (Straw + BC and Straw + Fh + BC) increased ^{13}C incorporation into total PLFAs (Fig. 2f) and altered the structure of the active microbial community (Fig. 5). This indicates that biochar stimulated the growth of active microorganisms and increased microbial utilization of straw.

The allocation of ^{13}C from straw to bacteria and fungi differed in the soils with and without biochar during straw decomposition (Fig. 2f), suggesting that microbial species possess distinct strategies for substrate utilization. *K*-strategists (mainly Gram + and fungi) mainly breakdown recalcitrant C compounds, whereas *r*-strategists (Gram −) mainly utilize labile C sources (Lu et al. 2017). As such, *K*-strategists are the main consumers of recalcitrant C in straw after labile C is exhausted; the input of aromatic C could also further increase the abundance of *K*-strategists (Liu et al. 2020). This was supported by the contents of ^{13}C-Gram + (a15:0, i15:0, i17:0, i16:0, and a17:0) and ^{13}C-fungi (16:1 w5c, 18:2 w6c, and 18:1 w9c), which were greater in the biochar-treated groups than in those without biochar after 28 days of incubation (Fig. 6b, c). Furthermore, the highest content of ^{13}C-fungi (18:1 w9c and 18:2 w6c) was observed in the Straw + BC group (Fig. 6b, c). Similarly, the abundance of fungi and their ability to utilize ^{13}C-labeled maize residues increased in the presence of biochar (Liu et al. 2020). This may be due to the fact that fungal mycelia can both efficiently transfer nutrients and water and colonize C sources with low bioavailability (e.g. biochar) and high C to N ratios (Cui et al. 2020). Thus, biochar input favors

fungal reproduction and growth. Furthermore, *K*-strategists are likely responsible for positive priming upon the depletion of labile C resources (Fontaine et al. 2003). Our RF model displayed that Gram + (i17:0, i16:0, and a17:0) and fungi (16:1 w5c and 18:1 w9c) mainly contributed to SOM mineralization (Figs. 4g and 6d). The regression analyses also discovered that the levels of Gram + and fungi decreased with DOC and NO_3^-, but increased with Olsen P (Additional file 1: Fig. S1, $p < 0.05$), suggesting that *K*-strategists satisfy their own growth by uptake of available C and N, which subsequently stimulates the microorganisms to acquire P from SOM, thus increasing the Olsen P level. Such an increase could fulfill microbial stoichiometric demands and facilitate microbial growth in typical P-limited rice soils (Heuck et al. 2015; Liu et al. 2022a). Hence, the alteration of the microbial population during straw decomposition was explained by fast-growth *r*-strategists that were replaced by a slow-growth *K*-strategists, which accumulate in recalcitrant fractions and nutrient-poor environments (Fig. 5). More specifically, and in line with the utilization preference of microorganisms, *r*-strategists preferentially utilized labile C sources within the straw (Blagodatskaya et al. 2007), whereas straw mineralization peaked before 28 days of incubation. In the last stage of straw decomposition, however, the content of *K*-strategists increased, and dominated SOM decomposition after exhaustion of soluble compounds in straw (Fang et al. 2018). This confirms that *K*-strategists (Gram + and fungi) are more competitive in the utilization of macromolecular compounds than *r*-strategists (Gram −).

During straw decomposition, a transition occurred among the microorganisms, shifting from *r*-strategists to *K*-strategists as available C sources depleted. The incorporation of biochar further influenced this microbial shift by improving the soil structure and nutrient content. Consequently, this fostered the colonization of *K*-strategists and expedited the mineralization of SOM. Biochar serves also as an electron shuttle in iron-rich flooded soils. The introduction of straw increases electron supply and thus facilitated electron transfer among microorganisms. This, in turn, promotes the reductive dissolution of unstable iron oxides, which accelerated the release of OC and nutrients from Fe-bound OC complexes. Consequently, this stimulation in the growth of active microorganisms accelerates SOM mineralization.

Overall, we investigated microbial mechanisms underlying straw-induced SOM mineralization after biochar application in flooded paddy soils by applying PLFA-SIP tools. We experimentally confirmed the role of *K*-strategists in SOM mineralization under simultaneous application of biochar and straw. We emphasize the importance of active microbial taxa, particularly Gram + bacteria

and fungi, in anaerobic iron-enriched soils mixed with biochar and straw and their contribution to SOM mineralization. Identifying key functional species specifically responding to the mixed incorporation of straw and biochar in anaerobic, iron-rich paddy soils should thus be prioritized. Such endeavors could greatly benefit from the utilization of isotope labeling and high-throughput sequencing techniques. Addition of substances in soil can directly or indirectly affect microorganisms. Straw inputs provide sufficient C sources for soil microorganism and increase microbial growth and activity. Straw inputs can indirectly affect microorganisms by improving soil aggregate structure and quality (Chen et al. 2022; Hu et al. 2021). Biochar application also directly modulates soil microbial activity and community structure through serving as a habitat or indirectly by altering soil redox processes and physico-chemical properties (e.g., biochar adsorptive characteristics can increase soil porosity and water-holding capacity) (Jaafar et al. 2014; Azeem et al. 2022). Indirect biochar or straw effects on microorganisms also depend on their feedstock and formation conditions (Deshoux et al. 2023; Luo et al. 2013). Consequently, the indirect effects of substances on microorganisms should be considered.

5 Conclusions

The intensity of SOM mineralization boosted by straw was dependent on biochar application. Straw provided sufficient C sources for microbial growth and activity, which greatly increased SOM mineralization. Biochar serves as a potential porous habitat for the growth of certain microbial groups (e.g., Gram+ and fungi) that are associated with nutrient acquisition. In the Fe-rich paddy soil, biochar also acted as an electron shuttle, accelerating Fe reduction and promoting the release of OC and nutrients from Fe (oxyhdr)oxides. Microbial activity increased with Olsen P but decreased with DOC and NO_3^- contents. Microbial composition was also dependent on biochar application. Therefore, in the late stage of straw decomposition, fungi and Gram+ bacteria dominated the decomposition of recalcitrant compounds in straw, whereas biochar addition further increased the abundance of fungi and Gram+, which subsequently accelerated SOM mineralization.

Supplementary Information

The online version contains supplementary material available at https://doi.org/10.1007/s42773-024-00312-7.

Additional file 1: Method S1. Preparation of ^{13}C-labeled rice straw. **Method S2.** Soil enzyme activities analysis. **Method S3.** Soil microbial phospholipid fatty acids (PLFA) extraction. **Figure S1.** Spearman correlation analysis of microbial biomarkers with soil properties and enzyme activities. Gram+, Gram-positive bacteria; Gram-, Gram-negative bacteria;

Act, Actinomycetes; Universal, non-specific microbial group. DOC, dissolved organic carbon; MBC, soil microbial biomass carbon. *p < 0.05, **p < 0.01, ***p < 0.001. **Figure S2**. Dynamics of key nutrients in response to ferrihydrite (Fh) and biochar (BC) addition to anaerobic paddy soil over a 70-day incubation period: (a) K_2SO_4-extracted dissolved organic carbon (DOC) from soil; (b) NH_4^+; (c) NO_3^-; (d) Olsen P; (e) Fe reduction; (f) soil pH. Straw, paddy soil with ^{13}C-labeled straw; Straw+BC, paddy soil mixed with ^{13}C-labeled straw and biochar; Straw+Fh, paddy soil mixed with ^{13}C-labeled straw and ferrihydrite; Straw+Fh+BC, paddy soil mixed with ^{13}C-labeled straw, ferrihydrite, and biochar. Values represent the means ± standard errors (n = 3), * indicate significant differences between amendments at the same point in time (*p < 0.05, **p<0.01, ***p<0.001); Na indicate no significant difference between treatments at each sampling period.

Data availability
Data will be made available on request.

Declarations

Competing interests
The authors state that they have no known financial conflict of interest or individual relationships that might affect the work presented here.

Author details
[1]State Key Laboratory for Managing Biotic and Chemical Threats to the Quality and Safety of Agro-Products, Key Laboratory of Biotechnology in Plant Protection of MARA and Zhejiang Province, Institute of Plant Virology, Ningbo University, Ningbo 315211, China. [2]Hubei Key Laboratory of Critical Zone Evolution, School of Earth Sciences, China University of Geosciences, Wuhan 430074, China. [3]School of Materials and Chemical Engineering, Ningbo University of Technology, Ningbo 315211, China. [4]School of Resources and Environmental Engineering, Jiangxi University of Science and Technology, Jiangxi 341000, China. [5]Department of Soil Science of Temperate Ecosystems, Department of Agricultural Soil Science, University of Goettingen, Goettingen 37077, Germany. [6]People Friendship University of Russia (RUDN University), Moscow 117198, Russia. [7]Institute of Environmental Sciences, Kazan Federal University, Kazan 420049, Russia.

References
Azeem M, Raza S, Li G, Simth P, Zhu Y (2022) Soil inorganic carbon sequestration through alkalinity regeneration using biologically induced weathering of rock powder and biochar. Soil Ecol Lett 4:293–306. https://doi.org/10.1007/s42832-022-0136-4

Bååth E, Anderson TH (2003) Comparison of soil fungal/bacterial ratios in a pH gradient using physiological and PLFA-based techniques. Soil Biol Biochem 35:955–963. https://doi.org/10.1016/S0038-0717(03)00154-8

Blagodatskaya EV, Blagodatsky SA, Anderson TH, Kuzyakov Y (2007) Priming effects in Chernozem induced by glucose and N in relation to microbial growth strategies. Appl Soil Ecol 37:95–105. https://doi.org/10.1016/j.apsoil.2007.05.002

Chen C, Dynes JJ, Wang J, Sparks DL (2014) Properties of Fe-organic matter associations via coprecipitation versus adsorption. Enviro Sci Technol 48:13751–13759. https://doi.org/10.1021/es503669u

Chen Z, Wang Y, Xia D, Jiang X, Fu D, Shen L, Wang H, Li QB (2016) Enhanced bioreduction of iron and arsenic in sediment by biochar amendment influencing microbial community composition and dissolved organic matter content and composition. J Hazard Mater 311:20–29. https://doi.org/10.1016/j.jhazmat.2016.02.069

Chen C, Hall SJ, Coward E, Thompson A (2020) Iron-mediated organic matter decomposition in humid soils can counteract protection. Nat Commun 11:2255. https://doi.org/10.1038/s41467-020-16071-5

Chen L, Sun S, Yao B, Peng Y, Gao C, Qin T, Zhou Y, Sun C, Quan W (2022) Effects of straw return and straw biochar on soil properties and crop growth: a review. Front Plant Sci 13:986763. https://doi.org/10.3389/fpls.2022.986763

Cooper RE, Eusterhues K, Wegner CE, Totsche KU, Küsel K (2017) Ferrihydrite-associated organic matter (OM) stimulates reduction by *Shewanella oneidensis* MR-1 and a complex microbial consortia. Biogeosciences 14:5171–5188. https://doi.org/10.5194/bg-14-5171-2017

Creamer CA, de Menezes AB, Krull ES, Sanderman J, Newton-Walters R, Farrell M (2015) Microbial community structure mediates response of soil C decomposition to litter addition and warming. Soil Biol Biochem 80:175–188. https://doi.org/10.1016/j.soilbio.2014.10.008

Cui J, Zhu Z, Xu X, Liu S, Jones DL, Kuzyakov Y, Shibistova O, Wu J, Ge T (2020) Carbon and nitrogen recycling from microbial necromass to cope with C:N stoichiometric imbalance by priming. Soil Biol Biochem 142:107720. https://doi.org/10.1016/j.soilbio.2020.107720

Dai Z, Barberan A, Li Y, Brookes PC, Xu J (2017) Bacterial community composition associated with pyrogenic organic matter (biochar) varies with pyrolysis temperature and colonization environment. mSphere 2:e00085-e117. https://doi.org/10.1128/mSphere.00085-17

Dai Z, Xiong X, Zhu H, Xu H, Leng P, Li J, Tang C, Xu J (2021) Association of biochar properties with changes in soil bacterial, fungal and fauna communities and nutrient cycling processes. Biochar 3:239–254. https://doi.org/10.1007/s42773-021-00099-x

Das S, Hendry MJ, Essilfie-Dughan J (2011) Transformation of two-line ferrihydrite to goethite and hematite as a function of pH and temperature. Environ Sci Technol 45:268–275. https://doi.org/10.1021/es101903y

de Boer W, Folman LB, Summerbell RC, Boddy L (2005) Living in a fungal world: impact of fungi on soil bacterial niche development. FEMS Microbiol Rev 29:795–811. https://doi.org/10.1016/j.femsre.2004.11.005

Deshoux M, Sadet-Bourgeteau S, Gentil S, Prevost-Boure NC (2023) Effects of biochar on soil microbial communities: a meta-analysis. Sci Total Environ 902:166079. https://doi.org/10.1016/j.scitotenv.2023.166079

Fang Y, Nazaries L, Singh BK, Singh BP (2018) Microbial mechanisms of carbon priming effects revealed during the interaction of crop residue and nutrient inputs in contrasting soils. Glob Chang Biol 24:2775–2790. https://doi.org/10.1111/gcb.14154

Fontaine S, Mariotti A, Abbadie L (2003) The priming effect of organic matter: a question of microbial competition? Soil Biol Biochem 35:837–843. https://doi.org/10.1016/S0038-0717(03)00123-8

Fu Y, Luo Y, Auwal M, Singh BP, Van Zwieten L, Xu J (2022) Biochar accelerates soil organic carbon mineralization via rhizodeposit-activated Actinobacteria. Biol Fertil Soils 58:565–577. https://doi.org/10.1007/s00374-022-01643-y

Ge T, Yuan H, Zhu H, Wu X, Nie S, Liu C, Tong C, Wu J, Brookes P (2012) Biological carbon assimilation and dynamics in a flooded rice––soil system. Soil Biol Biochem 48:39–46. https://doi.org/10.1016/j.soilbio.2012.01.009

Heuck C, Weig A, Spohn M (2015) Soil microbial biomass C:N:P stoichiometry and microbial use of organic phosphorus. Soil Biol Biochem 85:119–129. https://doi.org/10.1016/j.soilbio.2015.02.029

Hu Y, Sun B, Wu S, Feng H, Gao M, Zhang B, Liu Y (2021) After-effects of straw and straw-derived biochar application on crop growth, yield, and soil properties in wheat (Triticum aestivum l.) -maize (Zea mays l.) rotations: a four-year field experiment. Sci Total Environ 780:146560. https://doi.org/10.1016/j.scitotenv.2021.146560

Jaafar NM, Clode PL, Abbott LK (2014) Microscopy observations of habitable space in biochar for colonization by fungal hyphae from soil. J Integr Agric 13:483–490. https://doi.org/10.1016/S2095-3119(13)60703-0

Jeewani PH, Van Zwieten L, Zhu Z, Ge T, Guggenberger G, Luo Y, Xu J (2021) Abiotic and biotic regulation on carbon mineralization and stabilization in paddy soils along iron oxide gradients. Soil Biol Biochem 160:108312. https://doi.org/10.1016/j.soilbio.2021.108312

Jilling A, Keiluweit M, Gutknecht JLM, Grandy AS (2021) Priming mechanisms providing plants and microbes access to mineral-associated organic matter. Soil Biol Biochem 158:108265. https://doi.org/10.1016/j.soilbio.2021.108265

Jin Z, Shah T, Zhang L, Liu H, Peng S, Nie L (2020) Effect of straw returning on soil organic carbon in rice–wheat rotation system: a review. Food Energy Secur 9:1–13. https://doi.org/10.1002/fes3.200

Keiluweit M, Bougoure JJ, Nico PS, Pett-Ridge J, Weber PK, Kleber M (2015) Mineral protection of soil carbon counteracted by root exudates. Nat Clim Change 5:588–595. https://doi.org/10.1038/nclimate2580

Lal R (2004) Soil carbon sequestration impacts on global climate change and food security. Science 304:1623–1627. https://doi.org/10.1126/science.1097396

Lehmann J, Kleber M (2015) The contentious nature of soil organic matter. Nature 528:60–68. https://doi.org/10.1038/nature16069

Li Y, Hu S, Chen J, Müller K, Li Y, Fu W, Lin Z, Wang H (2018) Effects of biochar application in forest ecosystems on soil properties and greenhouse gas emissions: a review. J Soils Sediments 18:546–563. https://doi.org/10.1007/s11368-017-1906-y

Liu Z, Zhu M, Wang J, Liu X, Guo W, Zheng J, Bian R, Wang G, Zhang X, Cheng K, Liu X, Li L, Pan G (2019) The responses of soil organic carbon mineralization and microbial communities to fresh and aged biochar soil amendments. GCB Bioenergy 11:1408–1420. https://doi.org/10.1111/gcbb.12644

Liu Z, Wu X, Liu W, Bian R, Ge T, Zhang W, Zheng J, Drosos M, Liu X, Zhang X, Cheng K, Li L, Pan G (2020) Greater microbial carbon use efficiency and carbon sequestration in soils: amendment of biochar versus crop straws. GCB Bioenergy 12:1092–1103. https://doi.org/10.1111/gcbb.12763

Liu Q, Li Y, Liu S, Gao W, Shen J, Zhang G, Xu H, Zhu Z, Ge T, Wu J (2022a) Anaerobic primed CO_2 and CH_4 in paddy soil are driven by Fe reduction and stimulated by biochar. Sci Total Environ 808:151911. https://doi.org/10.1016/j.scitotenv.2021.151911

Liu Y, Shahbaz M, Fang Y, Li B, Wei X, Zhu Z, Lynn TM, Lu S, Shibistova O, Wu J, Guggenberger G, Ge T (2022b) Stoichiometric theory shapes enzyme kinetics in paddy bulk soil but not in rhizosphere soil. Land Degrad Deve 33:246–256. https://doi.org/10.1002/ldr.4141

Liu Y, Ge T, Wang P, van Groenigen XuX, Xu X, Cheng K, Zhu Z, Wang J, Guggenberger G, Chen J, Luo Y, Kuzyakov Y (2023) Residence time of carbon in paddy soils. J Clean Prod 400:136707. https://doi.org/10.1016/j.jclepro.2023.136707

Lu W, Liu N, Zhang Y, Zhou J, Guo Y, Yang X (2017) Impact of vegetation community on litter decomposition: Evidence from a reciprocal transplant study with ¹³C labeled plant litter. Soil Biol Biochem 112:248–257. https://doi.org/10.1016/j.soilbio.2017.05.014

Luo Y, Durenkamp M, De Nobili M, Lin Q, Devonshire BJ, Brookes PC (2013) Microbial biomass growth, following incorporation of biochars produced at 350 ℃ or 700 ℃, in a silty-clay loam soil of high and low pH. Soil Biol Biochem 57:513–523. https://doi.org/10.1016/j.soilbio.2012.10.033

Marschner P, Umar S, Baumann K (2011) The microbial community composition changes rapidly in the early stages of decomposition of wheat residue. Soil Biol Biochem 43:445–451. https://doi.org/10.1016/j.soilbio.2010.11.015

Mukherjee S, Mavi MS, Singh J, Singh BP (2020) Rice-residue biochar influences phosphorus availability in soil with contrasting P status. Arch Agron Soil Sci 66:778–791. https://doi.org/10.1080/03650340.2019.1639153

Nan Q, Xin L, Qin Y, Waqas M, Wu W (2021) Exploring long-term effects of biochar on mitigating methane emissions from paddy soil: a review. Biochar 3:125–134. https://doi.org/10.1007/s42773-021-00096-0

Palansooriya KN, Wong JTF, Hashimoto Y, Huang L, Rinklebe J, Chang SX, Bolan N, Wang H, Ok YS (2019) Response of microbial communities to biochar-amended soils: a critical review. Biochar 1:3–22. https://doi.org/10.1007/s42773-019-00009-2

Pan W, Kan J, Inamdar S, Chen C, Sparks D (2016) Dissimilatory microbial iron reduction release DOC (dissolved organic carbon) from carbon-ferrihydrite association. Soil Biol Biochem 103:232–240. https://doi.org/10.1016/j.soilbio.2016.08.026

Phillips DL, Newsome SD, Gregg JW (2005) Combining sources in stable isotope mixing models: alternative methods. Oecologia 144:520–527. https://doi.org/10.1007/s00442-004-1816-8

Sheng Y, Zhu L (2018) Biochar alters microbial community and carbon sequestration potential across different soil pH. Sci Total Environ 622–623:1391–1399. https://doi.org/10.1016/j.scitotenv.2017.11.337

Singh H, Northup BK, Rice CW, Prasad PVV (2022) Biochar applications influence soil physical and chemical properties, microbial diversity, and crop productivity: a meta-analysis. Biochar 4:8. https://doi.org/10.1007/s42773-022-00138-1

Su Y, Lv JL, Yu M, Ma ZH, Xi H, Kou CL, He ZC, Shen AL (2020) Long-term decomposed straw return positively affects the soil microbial community. J Appl Microbiol 128:138–150. https://doi.org/10.1111/jam.14435

Tian J, Dippold M, Pausch J, Blagodatskaya E, Fan M, Li X, Kuzyakov Y (2013) Microbial response to rhizodeposition depending on water regimes in paddy soils. Soil Biol Biochem 65:195–203. https://doi.org/10.1016/j.soilbio.2013.05.021

Wang H, Boutton TW, Xu W, Hu G, Jiang P, Bai E (2015) Quality of fresh organic matter affects priming of soil organic matter and substrate utilization patterns of microbes. Sci Rep 5:10102. https://doi.org/10.1038/srep10102

Wei L, Ge T, Zhu Z, Luo Y, Yang Y, Xiao M, Yan Z, Li Y, Wu J, Kuzyakov Y (2021) Comparing carbon and nitrogen stocks in paddy and upland soils: accumulation, stabilization mechanisms, and environmental drivers. Geoderma 398:115121. https://doi.org/10.1016/j.geoderma.2021.115121

Wei L, Ge T, Zhu Z, Ye R, Peñuelas J, Li Y, Lynn TM, Jone DL, Wu J, Kuzyakov Y (2022) Paddy soils have a much higher microbial biomass content than upland soils: a review of the origin, mechanisms, and drivers. Agric Ecosyst Environ 326:107798. https://doi.org/10.1016/j.agee.2021.107798

Wu J, Joergensen RG, Pommerening B, Chaussod R, Brookes PC (1990) Measurement of soil microbial biomass C by fumigation-extraction—an automated procedure. Soil Biol Biochem 22:1167–1169. https://doi.org/10.1016/0038-0717(90)90046-3

Wu L, Zhang W, Wei W, He Z, Kuzyakov Y, Bol R, Hu R (2019) Soil organic matter priming and carbon balance after straw addition is regulated by long-term fertilization. Soil Biol Biochem 135:383–391. https://doi.org/10.1016/j.soilbio.2019.06.003

Wu C, An W, Liu Z, Lin J, Qian Z, Xue S (2020) The effects of biochar as the electron shuttle on the ferrihydrite reduction and related arsenic (As) fate. J Hazard Mater 390:121391. https://doi.org/10.1016/j.jhazmat.2019.121391

Ye R, Doane TA, Morris J, Horwath WR (2015) The effect of rice straw on the priming of soil organic matter and methane production in peat soils. Soil Biol Biochem 81:98–107. https://doi.org/10.1016/j.soilbio.2014.11.007

Yu G-H, Kuzyakov Y (2021) Fenton chemistry and reactive oxygen species in soil: abiotic mechanisms of biotic processes, controls and consequences for carbon and nutrient cycling. Earth Sci Rev 214:103525. https://doi.org/10.1016/j.earscirev.2021.103525

Yu H-Y, Li F, Liu CS, Huang W, Liu T, Yu WM (2016) Iron redox cycling coupled to transformation and immobilization of heavy metals: implications for paddy rice safety in the red soil of South China. Adv Agron 137:279–317. https://doi.org/10.1016/bs.agron.2015.12.006

Yuan H, Zhu Z, Liu S, Ge T, Jing H, Li B, Liu Q, Lynn TM, Wu J, Kuzyakov Y (2016) Microbial utilization of rice root exudates: ^{13}C labeling and PLFA composition. Biol Fertil Soils 52:615–627. https://doi.org/10.1007/s00374-016-1101-0

Zelles L (1999) Fatty acid patterns of phospholipids and lipopolysaccharides in the characterisation of microbial communities in soil: a review. Biol Fertil Soils 29:111–129. https://doi.org/10.1007/s003740050533

Zhang H, Xu W, Li Y, Lyu J, Cao Y, He W (2017) Changes of soil microbial communities during decomposition of straw residues under different land uses. J Arid Land 9:666–677. https://doi.org/10.1007/s40333-017-0027-1

Zhang Y, Zheng N, Wang J, Yao H, Qiu Q, Chapman SJ (2019) High turnover rate of free phospholipids in soil confirms the classic hypothesis of PLFA methodology. Soil Biol Biochem 135:323–330. https://doi.org/10.1016/j.soilbio.2019.05.023

Zhou R, Tian J, Zhang F (2023) Microbial necromass within aggregates stabilizes physically-protected C response to cropland management. Front Agr Sci Eng 10:198–209. https://doi.org/10.15302/J-FASE-2023498.zhuzhulaos

Zhu Z, Ge T, Hu Y, Zhou P, Wang T, Shibistova O, Guggenberger G, Su Y, Wu J (2017) Fate of rice shoot and root residues, rhizodeposits, and microbial assimilated carbon in paddy soil—part 2: turnover and microbial utilization. Plant Soil 416:243–257. https://doi.org/10.1007/s11104-017-3210-4

Zhu Z, Fang Y, Liang Y, Li Y, Liu S, Li Y, Li B, Gao W, Yuan H, Kuzyakov Y, Wu J, Richter A, Ge T (2022) Stoichiometric regulation of priming effects and soil carbon balance by microbial life strategies. Soil Biol Biochem 169:108669. https://doi.org/10.1016/j.soilbio.2022.108669